ELSEVIER
Journal of Cystic Fibrosis 7 (2008) 197–205
Journal of Cystic Fibrosis
www.elsevier.com/locate/jcf

Upregulated expression of ENaC in human CF nasal epithelium

Nadine Bangel, Christoph Dahlhoff, Katja Sobczak, Wolf-Michael Weber *, Kristina Kusche-Vihrog

Institute of Animal Physiology, University of Muenster, Hindenburgplatz 55, 48143 Muenster, Germany

Received 12 February 2007; received in revised form 10 May 2007; accepted 27 July 2007
Available online 4 September 2007

Abstract

Cystic fibrosis (CF) is characterised by the absence of CFTR function resulting in a reduced Cl^- secretion and an increase in Na^+ absorption. This Na^+ hyperabsorption is mediated by the human amiloride-sensitive epithelial sodium channel (ENaC), but the underlying mechanisms are still unknown. After demonstrating functional differences of the Na^+ absorption in CF and non-CF epithelia in Ussing chamber experiments with human primary cultures, we compared ENaC sequences from CF and non-CF human nasal tissue (hnENaC), investigated the mRNA transcription levels *via* real-time PCR and studied the protein expression in Western blot analyses. We found no differences in the sequences of CF and non-CF hnENaC, but identified some polymorphisms. The real-time experiments revealed an enhanced mRNA amount of all three hnENaC subunits in CF tissue. By comparing the two groups on the protein level, we observed differences in the abundance of the Na^+ channel. While the α- and β-hnENaC protein amount was increased in CF tissue the γ-hnENaC was decreased. We conclude that the Na^+ hyperabsorption in CF is not caused by mutations in hnENaC, but by an increase in the transcription of the hnENaC subunits. This could be induced by a disturbed regulation of the channel in CF.

Keywords: ENaC; Cystic fibrosis; Na^+ hyperabsorption; Human nasal epithelia; Expression level; Real-time PCR

1. Introduction

Cystic fibrosis (CF) is a genetic disorder caused by a defect in the cystic fibrosis transmembrane conductance regulator (CFTR) gene, which encodes a chloride channel in epithelial cells. This defect results in ion transport abnormalities, which are characterised by a reduced Cl^- secretion and a markedly increased Na^+ absorption [1–3] mediated by the amiloride-sensitive epithelial sodium channel (ENaC). Substantial progress has been made to understand the function and regulation of CFTR. But since several years the Na^+ transport defect in CF patients due to ENaC has become focus of many studies. This channel is located in the apical membrane of epithelial cells and mediates the first step of sodium absorption in various organs, *e.g.* kidney, colon and lung [4]. ENaC is composed of three homologous subunits named α, β and γ, which together form the functional channels [5,6]. Additionally, a δ-subunit of ENaC was cloned from human brain [7]. The stoichiometry of ENaC is still a matter of discussion. Most groups propose a tetrameric structure [8,9], while others suggest that ENaC is formed by nine subunits [10,11]. However, the relation between structure and function has not been well defined so far. As a possible explanation for the excessive Na^+ absorption *via* ENaC a direct interaction with CFTR was postulated, which is known to be an important regulator of other proteins [12–15]. In the case of CF CFTR is not effectively inserted into the plasma membrane and the regulatory effect is no longer provided. Recently, it was shown that such a direct inhibitory effect of CFTR on ENaC does probably not exist [16].

The importance of human ENaC in Na^+ and fluid homeostasis is emphasised by the recent findings that mutations in the subunits are associated with different diseases. It was shown that some non-classical CF patients, who did not show any CFTR mutations, exhibited mutations in the β-ENaC subunit, associated with abnormal function of

* Corresponding author. Tel.: +49 251 83 21782; fax: +49 251 83 21785.
E-mail address: wmw@uni-muenster.de (W.-M. Weber).

1569-1993/$ - see front matter © 2007 European Cystic Fibrosis Society. Published by Elsevier B.V. All rights reserved.
doi:10.1016/j.jcf.2007.07.012

the ENaC protein [17]. Furthermore, it is known that mutations in the β- and γ-ENaC subunits lead to *e.g.* Liddle's syndrome [18,19] and pseudohypoaldosteronism (PHA I) [20]. PHA I shares some symptoms with CF such as elevated sweat electrolytes and *Pseudomonas aeruginosa* infections in the lung [21,22]. As a matter of fact, changes in the molecular structure of ENaC influence the function of the protein.

Furthermore, variations in the channel expression level may affect the Na^+ transport in epithelial cells. Recently, it was reported that an increase in β-ENaC expression in murine airway tissue evokes symptoms typically observed in CF lung disease [23]. Another hint for the involvement of transcriptional ENaC regulation in CF is the fact that β-ENaC mRNA is transiently increased in another murine model infected with *P. aeruginosa* [24]. These observations show that mutations in ENaC subunits and/or altered expression cause diverse dysfunctions in Na^+ absorption. So far, there is no adequate explanation for the functional upregulation of ENaC in CF epithelia or the mechanisms leading to this Na^+ hyperabsorption. However, all available data taken together, an upregulation of ENaC associated with an increased Na^+ absorption in CF epithelia can be postulated. To demonstrate the functional differences of the Na^+ absorption in CF and non-CF epithelia we performed Ussing chamber experiments with primary cultures of human nasal epithelia cells grown on permeable filters. These measurements confirm and extend previous findings of our group [3,25,26] that the amiloride-sensitive Na^+ absorption *via* ENaC in CF epithelia is significantly increased compared with non-CF epithelia *in vitro*. The underlying molecular mechanisms of this ENaC disorder are not known but it is possible that the differences in Na^+ transport in CF and non-CF tissue are due to structural variations of the channel. Therefore, we cloned and sequenced all three human nasal ENaC (hnENaC) subunits from CF and non-CF specimen and compared the nucleotide sequences. Since we identified no sequence abnormalities between CF and non-CF hnENaC, which might lead to an increased ENaC activity, we studied the mRNA expression of ENaC *via* quantitative real-time PCR (qRT-PCR). We observed an increase in mRNA expression levels of all three hnENaC subunits in CF tissue. Additionally, we determined the presence and abundance of hnENaC at the protein level and detected considerable differences in the expression pattern between CF and non-CF tissue. While α- and β-ENaC were increased, γ-ENaC protein expression was decreased in CF epithelia compared to non-CF tissue.

2. Materials and methods

2.1. Patients

We obtained nasal specimens from CF and non-CF patients undergoing nasal surgery. The samples were nasal polyps of patients suffering from chronic sinusitis. The study was approved by the committees for human studies of the University of Muenster (Ethik Kommission Muenster) and the University of Giessen (Ethik Kommission der Justus-Liebig-Universitaet Giessen). All patients gave informed consent.

For cloning and qRT-PCR experiments we combined four non-CF samples. To get precise values of the different individual CF patients these samples were not combined and used for relative comparison to the non-CF samples. For qRT-PCR experiments we analysed five patients homozygous for ΔF508 and one with a compound heterozygoty for ΔF508/R553X (also used for molecular cloning). For Western blot experiments we used four non-CF and two CF samples. All CF patients showed the full-blown clinical picture of cystic fibrosis.

2.2. Cell culture

Primary cell culture of the human nasal epithelium was performed as described before [27]. The CF and non-CF nasal epithelial cells were isolated by enzymatic digestion for 24–48 h and afterwards seeded on permeable collagen filters with a diameter of 14 mm (Cellagen TM dics CD 24, ICN Biomedicals, Costa Mesa, USA). The cells were cultured with serum-free F-12 Nutrient Mixture (Ham) (Invitrogen/Gibco, Karlsruhe, Germany) supplemented with the following agents: insulin (2 μg/ml) (Invitrogen/Gibco), epidermal growth factor (13 ng/ml) (Sigma, Deisenhofen, Germany), endothelial cell growth supplement (7.5 μg/ml) (Becton Dickinson GmbH, Heidelberg, Germany), triiodo-thyronine (3 nM) (Sigma), hydrocortisone (100 nM) (Sigma), gentamycin (10 μg/ml) (Biochrom AG, Berlin, Germany), penicillin/streptomycin (100 U/ml) (Invitrogen/Gibco), L-glutamin (2 mM) (Invitrogen/Gibco) and transferrin (4 μg/ml) (Invitrogen/Gibco). Previously, it was shown that these supplements had no effect on the electrical parameters of the human nasal epithelium [25]. Cells were incubated in 95% air and 5% CO_2 at 37 °C. 7–9 days after seeding the cells on the membrane, we normally obtained confluent monolayers and proceeded with Ussing chamber measurements.

2.3. Transepithelial measurements

After reaching confluence, the nasal epithelial cells were mounted in modified Ussing chambers designed by Prof. Willy Van Driessche (KU Leuven, Belgium). The two compartments of the Ussing chamber were continuously perfused with cell culture Ringer at 37 °C. Voltage and current electrodes (AgCl wires) were used and were electrically connected to the chamber by KCl-agar bridges. The current electrodes held the transepithelial potential (V_t), which is established by an active transport of ions to zero. The required current of compensation, called short circuit current (I_{sc}), depends on changes in conductance of the epithelium, which is generated by perfusion of different solutions. I_{sc} was continuously monitored using the computer program ImpDsp1.4 (Prof. Willy Van Driessche).

The measured area had a size of 0.5 cm^2, while the electrical parameters were normalised to an area of 1 cm^2.

2.4. Solutions

Cell culture Ringer was composed as follows: 130 mM NaCl, 5 mM KCl, 1 mM $CaCl_2$, 2 mM $MgCl_2$, 5 mM glucose, 10 mM HEPES. In the Na^+-free solution used, NaCl was replaced by an equivalent amount of TMACl (tetramethylammonium chloride). For investigation of the amiloride-sensitive currents through ENaC the apical compartment of the Ussing chamber was perfused with amiloride (100 μM) in cell culture Ringer.

2.5. Extraction of RNA

Total RNA was extracted from human CF and non-CF nasal polyps following the standard protocol of RNeasy Mini kit plus (Qiagen, Hilden, Germany). In this procedure the genomic DNA contamination was effectively removed with a gDNA Eliminator spin column, so that additional DNase digestion was not necessary. Afterwards, the RNA was eluted in 30 μl RNase-free water.

The concentration of RNA was determined by absorbance measurement at 260 nm (A_{260}) in a spectrophotometer using UV cuvettes. The integrity and size distribution of total RNA was analysed *via* denaturing agarose gel electrophoresis and ethidium bromide staining. To check the RNA quality 1.5 μg total RNA was loaded per lane.

2.6. cDNA synthesis

Total RNA (1 μg) was used to generate first-strand cDNA by using the SuperScript II reverse transcriptase kit (Invitrogen) and oligo (dT) primers. Finally, cDNA was diluted 1:10 prior to use in qRT-PCR.

2.7. Molecular cloning of CF and non-CF α-, β-, γ-hnENaC cDNA

After PCR amplification with specific oligonucleotide primers for the three subunits according to the published sequences of human ENaC (http://www.ncbi.nih.gov), all expected distinct bands were excised using the QIAquick Gel Extraction kit (Qiagen) and cloned into the pCR®II-TOPO TA vector (Invitrogen). Since no full-length clones for the α-hnENaC and γ-hnENaC could be amplified, the 3′ end of the α-hnENaC cDNA was obtained applying the protocol for rapid amplification of cDNA ends (RACE) following the suppliers directions (Invitrogen). 5′ RACE assays were carried out for the α- and γ-hnENaC subunits with a series of nested oligonucleotide primers using the 5′ RACE kit (Invitrogen). Products of those PCR reactions were also cloned in the pCR®II-TOPO TA vector. Full-length β-hnENaC was generated using two specific primers overlapping the untranslated region and the coding sequence (5′-GCC CGA GCA GGT GCC ACT ATG C-3′and 5′-GGT GGA CAG GGG CAG GGT TAG ATG-3′). The nucleotide sequences of non-CF α-, β-, γ-hnENaC cDNA were submitted to GenBank, accession numbers DQ402522 (α-hnENaC), DQ402523 (β-hnENaC) and DQ402524 (γ-hnENaC).

2.8. Sequence data analysis

For cDNA sequence analysis and molecular weight prediction of the amino acid sequences we used the tools provided by the ExPasy Molecular Biology Server of the Swiss Institute of Bioinformatics (http://www.expasy.ch) and the National Centre for Biotechnology Information (http://www.ncbi.nlm.nih.gov). All clones were commercially sequenced by GENterprise (GENterprise GmbH, Mainz, Germany). The complete α-, β- and γ-hnENaC amino acid sequences of CF and non-CF tissue were added to a multi-sequence alignment by using GENEDOC 2.6.

2.9. Quantitative real-time PCR with SYBR® Green I

For qRT-PCR experiments cDNA was generated as described before. We combined the cDNA from four non-CF patients to avoid statistical spreading in this control tissue. The oligonucleotide primers for qRT-PCR were selected to bind specifically to human cDNA and created spanning exon/exon boundaries to prevent amplification of genomic DNA. All selected specific primers (Table 1) produce a PCR-fragment in the range of 100 bp.

For qRT-PCR we used the iQ5 Real-Time PCR Detection System (Biorad, Munich, Germany) and the iQ™ SYBR® Green Supermix (Biorad). Optimal reaction conditions were obtained with 12.5 μl 2x iQ™ SYBR® Green Supermix (100 mM KCl, 40 mM Tris HCl, pH 8.4, 0.4 mM of each dNTP (dATP, dCTP, dGTP and dTTP), i*Taq* DNA polymerase 50 units/ml, 6 mM $MgCl_2$, SYBR® Green I, 20 nM fluorescein and stabilizers), 5 μM of each primer and 4 μl of the diluted cDNA in a total volume of 25 μl. Amplifications were performed starting with a 2 min template denaturation step at 95 °C followed by 45 cycles of denaturation at 95 °C for 10 s and a combined primer annealing/extension at the gene specific primer temperature (60 °C) for 30 s. At the end of each PCR a melting curve with increasing temperature from 60 °C to 95 °C in steps of 3 °C min^{-1} was generated. The fluorescence increase was automatically measured every 10 s to detect fluorescence-alteration and to confirm the specificity of the amplification. To determine the primer-efficiency a 1:5 dilution series was performed with non-CF cDNA as template. All samples were amplified in triplicate and the C_T values were obtained for further calculations.

2.10. Real-time PCR data analysis

The data were analysed using the iCycler iQ Software Version 3.1 (Biorad). This software determines the threshold

Table 1
Nucleotide sequences of primers used in quantitative real-time RT-PCR

Targets	Sequences 5′-3′	Amplicon length (bp)	T_m (° C)
α-hnENaC	CCTCTGTCACGATGGTCACCCTCC	113	60
	CTGAGCTCGTCTTTGACCTGCTG		60
β-hnENaC	CCAATATCACCCTGAGCAGGAAGGG	112	60
	CAATAACATCGTCTGGCTGCTCTCG		61
γ-hnENaC	GAGCCCAGCCAACAGTATTGAGATG	93	59
	CTCTGTTGTCTGCGTCATCGAGATC		60
h-GAP-DH	CATCACCATCTTCCAGGAGCGAG	109	59
	CACCACCATGGAGAAGGCTGGGG		60
h-β-Actin	CCTGGAGAAGAGCTACGAGCTG	107	60
	CCTTCCTTCCTGGGCATGGAGTC		59
h-PolRIIa	CTTGTGTGATACCATGACCTGTCGTG	115	60
	CCTTTGAGGAAACGGTGGACGTGC		60

T_m, melting temperature.

cycle (C_T) for expression-analysis, which always appears during the exponential phase of the PCR. For the relative quantification the obtained C_T-values were normalised with three housekeeping genes (HKG) as reference index. As HKG we used a structure-related gene (human β-Actin), a metabolism-related gene (human GAP-DH) and a transcription-related gene (human PolRIIa). The normalisation was reached by means of the REST©-Software (Relative Expression Software Tool V1.9.9©2005, Corbett Research Pty. Ldt.). The used mathematical model is based on the PCR-efficiency and the mean threshold cycle deviation [28,29].

2.11. Protein biochemistry

Membrane proteins from human nasal epithelium were isolated using lysis buffer (1 mM Tris ,15 mM NaCl, 0.2 mM EDTA, 2% Triton X-100) and a protease inhibitor cocktail (10 mM Leupeptin, 1 mg/ml Trypsininhibitor, 25 μM Pefablock, 100 mM PMSF) was added to this detergent mixture. It was shown that 2% Triton X-100 is sufficient to solve all of the intracellular and cell surface pools of the sodium channel ENaC [30]. The extracts were homogenised with a Sonifier®ultrasonic cell disrupter (Branson, Danbury, USA) and centrifuged for 30 min at 4,000 g at 4 °C to remove insoluble material. The concentration of the proteins in the supernatant was measured photometrically using the Bradford test [31]. For the detection of the α- and β-ENaC subunits 10 μg and for the γ-ENaC subunit 20 μg of total membrane proteins were separated *via* SDS-PAGE (7.5% acrylamide) and transferred to a PVDF membrane. Non-specific binding sites were blocked for 2 h with 5% nonfat dry milk in Tris-buffered saline/Tween (TBST: 10 mM Tris HCl, pH 7.4; 140 mM NaCl; 0.3% Tween 20). The ENaC α- and γ-subunit were detected with a rabbit anti α-ENaC and a rabbit anti γ-ENaC antibody (Dianova, Hamburg, Germany), respectively with a concentration of 1:2,500 diluted in 5% nonfat dry milk/TBST overnight at 4 °C. The ENaC β-subunit was detected with a rabbit anti β-ENaC antibody (Santa Cruz, California, USA) with a concentration of 1:100 diluted in 1% nonfat dry milk/TBST overnight at 4 °C. After washing in TBST the membrane was incubated for 1 h at room temperature with the goat anti-rabbit IgGs conjugated with alkaline phosphatase (Dianova) diluted 1:10,000 in 5% nonfat dry milk/TBST for the α- and γ-subunit and with the goat anti-rabbit IgGs conjugated with alkaline phosphatase (Santa Cruz) diluted 1:10,000 in 1% nonfat dry milk/TBST for the β-subunit. The membrane was washed again in TBST and detection was carried out with NBT (nitroblue tetrazolium) and BCIP (5-bromo-4-chloro-3-indolyl phosphate).

2.12. Densitometric evaluation of Western blots

The transferred PVDF membranes were digitally scanned and protein bands were semi-quantitatively analysed by densitometry using ImageJ analysis software 1.36 [32]. We calculated the areas of the detected bands from the CF and non-CF samples. These values were given as *x*-fold alteration according to the α-, β- and γ-hnENaC subunit abundance. For demonstration the non-CF samples were set as control and therefore, normalised to 1.0 (100%).

2.13. Statistics

Where applicable, data are expressed as arithmetic means ± SEM; *n* is the number of experiments. Statistical analysis was made by the *t*-test where appropriate, and a significant difference was assumed at $p < 0.001$.

3. Results

3.1. Transepithelial measurements

With electrophysiological measurements in modified Ussing chambers we showed *in vitro* that the amiloride-sensitive Na^+ absorption *via* ENaC in human nasal CF primary cultured cells was significantly increased compared

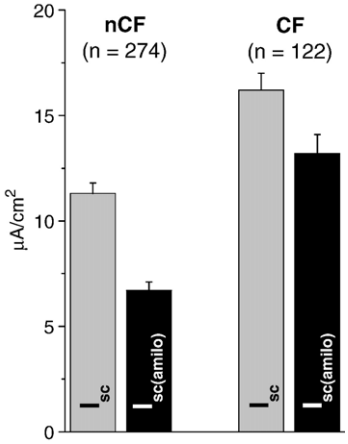

Fig. 1. Total short circuit current (I_{sc}, light grey bars) and amiloride-sensitive short circuit current mediated by ENaC ($I_{sc(amilo)}$, black bars) in non-CF (nCF) and CF human nasal primary cultured cells. The number of preparations is given in brackets. The results are different at a significance level of $p < 0.001$.

to cells derived from non-CF tissue. A large portion of the total transepithelial current (I_{sc}) could be inhibited by amiloride. This amiloride-sensitive current ($I_{sc(amilo)}$) is mediated by ENaC. I_{sc} in CF epithelia was increased by ~40% (Fig. 1, grey bars). However, $I_{sc(amilo)}$ mediated by ENaC was nearly doubled in CF epithelia (Fig. 1, black bars). Interestingly, almost the complete transepithelial current in CF epithelia was mediated by ENaC while in non-CF epithelia around half of total I_{sc} was mediated by amiloride-insensitive Na^+ conductances, which are not identified so far.

3.2. Cloning of α-, β- and γ-hnENaC from CF and non-CF epithelia

The quality of total RNA was proven for each experimental approach. The agarose gel showed the human 28 S and 18 S rRNA bands that confirmed the correct ratio of 2:1 and no contaminating DNA or RNA degradation products.

We cloned and sequenced all three hnENaC subunits from CF and non-CF tissue and compared the amino acid sequences in a multi-sequence alignment with each other. We found no sequence differences between CF and non-CF hnENaC. The general properties like the calculated molecular weight and nucleotide sequence length (α-ENaC: 2010 bp; β-ENaC: 1923 bp; γ-ENaC: 1950 bp) are in agreement with the previously published properties of hENaC (http://www.ncbi.nlm.nih.gov). The sequences of the full-length non-CF α-, β- and γ-hnENaC cDNA were submitted to GenBank, those of CF α-, β- and γ-hnENaC are equal to the non-CF sequences (100% homology).

Furthermore, we detected single nucleotide polymorphisms (SNP) within both sequences of CF and non-CF hnENaC in comparison with already published sequences (Table 2).

3.3. Quantitative real-time PCR

Quantitative real-time PCR was used to examine the RNA transcription levels of CF and non-CF hnENaC subunits. The different RNA transcription levels were determined *via* relative quantification of the obtained C_T values calculated by the REST© software. The C_T is defined as the number of cycles needed for the fluorescence to reach a specific threshold level of detection and is inversely correlated with the amount of template nucleic acid present in the reaction [33]. We compared the expression of the α-, β- and γ-hnENaC subunits in the nasal epithelium of six CF-patients relative to the expression of a combined compilation of four non-CF patients normalised to 1.0 (Fig. 2). Although the subunit composition slightly oscillated for every individual patient, we found that the amount of the α-, β- and γ-hnENaC mRNA expression in human nasal CF tissue is obviously increased compared to non-CF tissue. For a descriptive demonstration of each measured CF specimen we averaged the obtained data. We observed that the α-hnENaC gene of the CF group showed a 1.7-fold increase in the mRNA transcription level compared with the combined non-CF group. The β-hnENaC mRNA expression in CF tissue is even 3.3-fold enhanced on average compared with the control group. Furthermore, we found an averaged 3.4-fold increase in γ-hnENaC mRNA expression in CF tissue as compared with non-CF tissue. The values of each individual are partially increased. One CF patient (CF specimen 3) revealed a 5.96-fold increased β-hnENaC subunit expression, while another CF patient (CF specimen 6) showed a 4.7-fold increase for this subunit. Insofar, these individual values exceeded the average of 3.2-fold for the β-hnENaC subunit nearly twice. We found a similar situation for

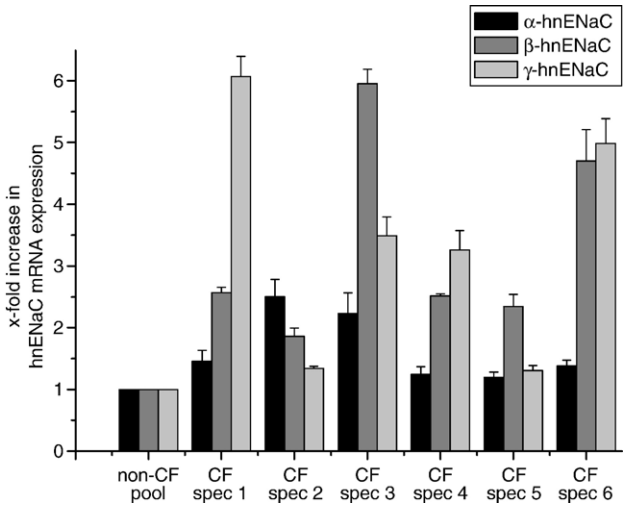

Fig. 2. mRNA expression data for all three hnENaC subunits of CF patients. Data were acquired by real-time PCR and are shown as *x*-fold increase± SEM of mRNA expression for each subunit and CF patient, respectively. Relative mRNA expression of the combined non-CF population was normalised to 1.0 (100%). α-hnENaC mRNA expression is marked by a black column for CF specimen 1: 1.46-fold±0.17; for CF specimen 2: 2.5-fold±0.28; for CF specimen 3: 2.23-fold±0.33; CF specimen 4: 1.25-fold±0.12; for CF specimen 5: 1.20-fold±0.08; for CF specimen 6: 1.38-fold±0.09. The β-hnENaC mRNA expression is displayed by a dark grey column for CF specimen 1: 2.57-fold±0.09; for CF specimen 2: 1.86-fold±0.13; for CF specimen 3: 5.96-fold±0.23; CF specimen 4: 2.51-fold±0.04; for CF specimen 5: 2.34-fold±0.20; for CF specimen 6: 4.70-fold±0.51. The γ-hnENaC mRNA expression is represented by a light grey column for CF specimen 1: 6.07-fold±0.33; for CF specimen 2: 1.34-fold±0.03; for CF specimen 3: 3.49-fold±0.31; CF specimen 4: 3.26-fold±0.32; for CF specimen 5: 1.31-fold±0.08; for CF specimen 6: 4.99-fold±0.40.

Table 2
Single nucleotide polymorphisms in the α-, β- and γ-hnENaC subunits from CF and non-CF tissue and appropriate references

α-ENaC	Reference	β-ENaC	Reference	γ-ENaC	Reference
T663A	[53,54]	A314G	[55]	R178W	[53,55,56]
				P502A	
				A614S	
		A336P	[53,56]		
				F339S	[55]
				A350T	
				Y369S	
				D375G	
				S458R	

samples of γ-hnENaC subunit: two CF patients showed drastically enhanced amounts of the γ-hnENaC mRNA (CF specimen 1: 6.07-fold; CF specimen 6: 4.99-fold) that are almost twice as much as the mean (3.5-fold) increase for the γ-hnENaC subunit, respectively. The exact individual values of each hnENaC subunit and each CF patient are shown in Fig. 2 and listed in Table 3.

3.4. Protein biochemistry

In order to determine the presence and abundance of hnENaC protein in CF and non-CF control tissue we carried out immunoblotting experiments. SDS-PAGE analyses showed the existence of one distinct α-hnENaC band in the range of 66 kDa. Additionally, the anti α-ENaC antibody detected a second distinct band in the range of 55 kDa in CF and non-CF tissue. Before, this antibody was also tested in Western blot experiments with proteins isolated from ENaC expressing oocytes, where it recognised one distinct ENaC band. Since we used protease inhibitors for the protein purification and highly specific antibodies, the second protein band is not due to proteolytic cleavage during the preparation or cross-reaction of the antibody. The 66 kDa band and the 55 kDa α-hnENaC specific fragment could represent an endogenous proteolytic cleaved form of the α-hnENaC protein.

The anti β-ENaC antibody bound to one specific band in the range of 73 kDa, and with the anti γ-ENaC antibody we identified a specific band of approximately 74 kDa. The molecular weights of the β- and γ-hnENaC subunits were in agreement with the calculated and previously published data of these unprocessed proteins (http://www.ncbi.nlm.nih.gov). For the densitometric determination we digitised the Western blots and quantified the amount of hnENaC protein using the ImageJ program 1.36 [32]. We found apparent differences in the protein expression pattern between CF and non-CF tissue. Although, we observed no detectable differences between the 66 kDa band from CF and non-CF tissue, the second lower α-hnENaC band was 5-fold increased in CF tissue. The abundance of the CF β-hnENaC subunit was also 3.5-fold enhanced as compared with non-CF samples. In contrast to these observations, the quantity of the γ-hnENaC protein was 4-fold decreased in CF epithelia as compared with non-CF tissue. Fig. 3A shows representative Western blots for all three subunits, and the densitometric evaluation of the specific hnENaC bands is shown in Fig. 3B.

Table 3
Individual hnENaC mRNA expression level of each CF patient compared with the non-CF control group (normalised to 1.0)

No. of CF patient	α-hnENaC (*x*-fold increase)	β-hnENaC (*x*-fold increase)	γ-hnENaC (*x*-fold increase)
CF tissue specimen 1	1.46±0.17	2.57±0.09	6.07±0.33
CF tissue specimen 2	2.50±0.28	1.86±0.13	1.34±0.03
CF tissue specimen 3	2.23±0.33	5.96±0.23	3.49±0.31
CF tissue specimen 4	1.25±0.12	2.51±0.04	3.26±0.32
CF tissue specimen 5	1.20±0.08	2.34±0.20	1.31±0.08
CF tissue specimen 6	1.38±0.09	4.70±0.51	4.99±0.40

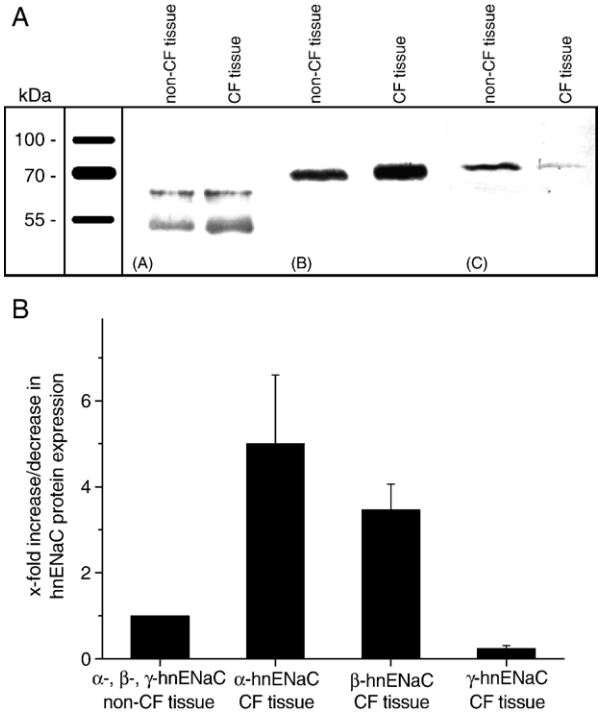

Fig. 3. (A) Western Blots of the three hnENaC subunits from CF and non-CF tissue. Total membrane proteins from human nasal CF and non-CF tissue were isolated using 2% Triton X-100 and separated on a 7.5% SDS-PAGE. To identify ENaC we used specific anti-ENaC antibodies against the subunits. We detected two specific bands of α-ENaC in the range of 66 and 55 kDa in the non-CF control and the CF tissue, respectively (A), one specific band of β-ENaC in the range of 73 kDa (B) and a γ-ENaC specific band in the range of 74 kDa (C).(B) Semi-quantitative protein expression of hnENaC in CF and non-CF tissue. Expression of hnENaC α-, β- and γ-protein was studied in normal (non-CF) and CF nasal polyps by Western blotting and quantified by densitometry using ImageJ 1.36. We found a 5±1.6-fold increase of the α-hnENaC protein ($n=5$), a 3.5±0.6-fold increase of the β-hnENaC ($n=6$) and a 4-fold (0.24±0.07) decrease of the γ-hnENaC protein ($n=5$) in CF tissue compared with the non-CF tissue. Relative protein expression of the non-CF hnENaC control protein was normalised to 1.0 (100%).

4. Discussion

ENaC is involved in the airway symptoms of CF due to its hyperactivity resulting in an accelerated Na^+ absorption and an increase in lung mucus viscosity. In respect to the changes in the mucus of CF patients, two opposing hypothesis concerning the ionic composition of the airway surface liquid (ASL) are discussed: (i) the hypotonic theory (ASL/defensin hypothesis) postulates that normal airway epithelia are covered by an ASL with a low NaCl concentration, which enables the inflammatory response and defence against bacteria. (ii) The other hypothesis (the isotonic volume transport/mucus clearance hypothesis) deals with the ion transport functions of CFTR and links the defects in ion

transport in CF to the initiation of the lung symptoms [34,35]. Jayaraman et al. investigated airway surface liquid height and found no evidence for active ion transport regulating ASL height in tracheal epithelia [36]. In contrast, in many studies it was demonstrated that an unbalanced ion composition of the mucus lining the airways due to malfunction of CFTR and ENaC is responsible for the lung symptoms of CF patients [23,35]. CF epithelia are characterised by a markedly increased Na^+ uptake *via* ENaC. In this study we confirm and substantially extend previous findings from primary cultured cells [3] demonstrating that the total transepithelial short circuit current (I_{sc}) across CF respiratory epithelia is increased by about 40% while the amiloride-sensitive Na^+ uptake *via* ENaC ($I_{sc(amilo)}$) is nearly doubled *in vitro*. In CF nasal epithelia Na^+ absorption mediated by ENaC represents the major part in total epithelial ion transport. Therefore, we set out to explore the molecular mechanisms underlying that strong Na^+ hyperabsorption in CF epithelia.

There are many hypotheses dealing with the hyperactivity of ENaC. It is possible that either the molecular structure of the ENaC genes is modified or that the regulation or interaction with CFTR and the channel is biased. However, due to the lack of an appropriate mouse model reproducing the human CF airway epithelial phenotype, it is very difficult to study the situation *in vivo*. In the present study we used human nasal tissue as a well-established cell model system [26,37] to investigate the hnENaC in CF and non-CF epithelia *in vitro*. Thus, we compared the molecular sequences of CF and non-CF hnENaC, and investigated mRNA and protein levels of CF and non-CF hnENaC. In a multi-sequence alignment of the six nucleotide hnENaC sequences no differences between CF and non-CF tissue were observed. These results indicate that the Na^+ hyperabsorption *via* ENaC in CF epithelia is not due to structural modifications or mutations of the ENaC genes. However, we found some gene polymorphisms, which have been described previously for human ENaC derived from other tissues. We identified a common T663A polymorphism within the C-terminus of the hnENaC α-subunit of CF and non-CF epithelia. Furthermore, polymorphisms in the β- and γ-hnENaC subunits have been detected. Since all polymorphisms are present in both CF and non-CF hnENaC these changes in the nucleotide sequences are not sufficient to explain the drastic Na^+ hyperabsorption in CF.

To prove the hypothesis that the increased Na^+ absorption in CF airways could be due to an enhanced expression of hnENaC, we compared the mRNA expression levels of hnENaC derived from non-CF and CF epithelia using qRT-PCR. Indeed we observed an increase in the mRNA levels of all three hnENaC subunits in CF tissue compared with the non-CF samples. These results show for the first time a direct correlation between cystic fibrosis and the mRNA level of hnENaC. In this context it is obvious that mainly the regulatory subunits of ENaC, the β- and the γ-subunit [5], are elevated. This fact could indicate that in CF the regulation of the ion channel itself is modified. However, the upregulation of hnENaC might be associated with the functional amiloride-sensitive Na^+ hyperabsorption in CF tissue, which was shown in several studies [1,3]. The molecular mechanisms leading to the increase in ENaC mRNA transcription are still unknown.

By comparing hnENaC between CF and non-CF tissue at the protein level we found remarkable differences in the protein expression: the α- and β-ENaC subunits are increased in CF tissue while the γ-ENaC subunit is decreased. The specific anti α-ENaC antibody detected two distinct protein bands in CF and non-CF tissue, only one being increased in all CF samples. Previously, it was demonstrated that ENaC undergoes extensive post-translational processing by proteolytic cleavage and glycosylation [38,39]. This processing may result in tissue specific protein bands with varying molecular weights. Recently, a compilation of the molecular weights of ENaC from different cell types and tissues was published [40]. In addition to the increased mRNA level the changes in protein expression of hnENaC found in CF tissue indicate that the regulation or post-translational processes in CF could be modified.

In the pathogenesis of CF, infections with pathogens, inflammation, changes in protease activity or impaired regulation by defect CFTR are described [41,42]. Furthermore, mediators of the immune response like cytokines could influence the transcriptional processes. For example, the lack of CFTR leads to abnormal function of transcription factors, which regulate the synthesis of the pro-inflammatory cytokines and chemokines elevated in CF (reviewed by [43]). It was shown that the colonisation of the viscous mucus lining the respiratory epithelia of CF patients with the pathogen *P. aeruginosa* affects the transcription of the three ENaC subunits and a transiently increased β-ENaC mRNA expression [24]. Other pathogens, which colonise CF epithelia in the lung like *Staphyloccocus aureus* might also play an important role in this context [44]. Thus, the chronic infections of the CF patients could cause the changes in the expression of ENaC. Taken together, all these factors might modulate the regulation of hnENaC mRNA and protein expression. However, no direct correlation between mRNA transcription and protein level was found. In this context May et al. showed that changes on the mRNA level might not strictly reflect changes at the protein level and *vice versa* [45].

We hypothesise that the differences in the protein expression between CF tissue and the control group could indicate a modified hnENaC subunit composition in CF epithelia. It was demonstrated that the expression level of each subunit is markedly different in various Na^+ absorbing epithelia and that single channel conductances are dependent on the subunit composition of ENaC. Furthermore, it is known that changes in the stoichiometry of heteromultimeric proteins, *e.g.* ENaC, lead to different functional properties [46]. The expression of the three ENaC subunits seems to vary considerably between different tissues. It was shown that some cells in the lung express only the α- and γ-ENaC subunits [47]. In colon and kidney the expression of the three ENaC subunits extremely depends on the stimulation by

aldosterone [48,49]. Additionally, one group showed *via* immunological and electrophysiological methods very rapid changes in the processing and maturation of the channels in rat kidney which could be due to a daily regulation of ENaC activity and Na^+ reabsorption [50]. Therefore, it is likely that the hnENaC subunit composition in CF tissue is indeed altered and the physiological properties are changed. The combination of an increase in hnENaC transcription and a modified stoichiometry might explain Na^+ hyperabsorption in CF. Taken together, in this study we found for the first time strong evidence that hnENaC in CF tissue is markedly increased at the mRNA and protein level compared with non-CF samples. This could be due to a modified hnENaC regulation resulting in channels with modulated physiological properties and an elevated Na^+ absorption. Since cells derived from human nasal epithelium have been reliable and useful tools for the study of ion transport defects related to CF *in vitro* [26,37], these results are important for ongoing CF therapies. According to the amiloride/benzamil therapy which decreased the Na^+ absorption [51,52] long-lasting suppression of ENaC transcription with highly specific antisense oligonucleotides (Weber et al., unpublished data) can be developed.

Acknowledgement

We thank Prof. Dr. Claudia Rudack (HNO-Klinik, University of Muenster), Claudia Rückes-Nilges (Kinderklinik, Justus Liebig University, Giessen) and Dr. Hartmut Winzer (Maria-Josef-Hospital, Greven) for kindly providing us with human nasal specimen. We are grateful for the support and availability of the real-time experiment set-up by Stefan Weinl, member of the working group of Prof. Dr. Jörg Kudla (University of Muenster). We are grateful to Dr. Nina Ullrich (Imperial College London) and Dr. Frank Nunes (University of Muenster) for discussions. Parts of the work were supported by Mukoviszidose e.V. Giessen and Deutsche Fördergesellschaft zur Mukoviszidoseforschung.

References

[1] Boucher RC, Stutts MJ, Knowles MR, Cantley L, Gatzy JT. Na^+ transport in cystic fibrosis respiratory epithelia. J Clin Invest 1986;78:1245–52.
[2] Boucher RC, Cotton CU, Gatzy JT, Knowles MR, Yankaskas JR. Evidence for reduced Cl and increased Na permeability in cystic fibrosis human primary cell cultures. J Physiol (Lond) 1988;405:77–103.
[3] Rückes-Nilges C, Weber U, Lindemann H, Münker G, Clauss W, Weber W-M. Minor role of Cl^- secretion in non-cystic fibrosis and cystic fibrosis human nasal epithelium. Cell Physiol Biochem 1999;9:1–11.
[4] Garty H, Palmer LG. Epithelial sodium channels: function, structure, and regulation. Phys Rev 1997;77:359–96.
[5] Alvarez de la Rosa D, Canessa CM, Fyfe GK, Zhang P. Structure and regulation of amiloride-sensitive sodium channels. Annu Rev Physiol 2000;62:573–94.
[6] Canessa CM, Schild L, Buell G, Thorens B, Gautschi I, Horisberger J-D, et al. Amiloride-sensitive epithelial Na^+ channel is made of three homologous subunits. Nature 1994;367:463–7.
[7] Waldmann R, Champigny G, Bassilana F, Voilley N, Lazdunski M. Molecular cloning and functional expression of a novel amiloride-sensitive Na^+ channel. J Biol Chem 1995;270:27411–4.
[8] Firsov D, Gautschi I, Merillat A-M, Rossier BC, Schild L. The heterotetrameric architecture of the epithelial sodium channel (ENaC). EMBO J 1998;17:344–52.
[9] Kosari F, Sheng S, Li J, Mak D-OD, Foskett JK, Kleyman TR. Subunit stoichiometry of the epithelial sodium channel. J Biol Chem 1998;273:13469–74.
[10] Snyder PM, Cheng C, Prince LS, Rogers JC, Welsh MJ. Electropyhsiological and biochemical evidence that DEG/ENaC cation channels are composed of nine subunits. J Biol Chem 1998;273:681–4.
[11] Staruschenko A, Adams E, Booth RE, Stockand JD. Epithelial Na^+ channel subunit stoichiometry. Biophys J 1998;88(6):3966–75.
[12] Mall M, Hipper A, Greger R, Kunzelmann K. Wild type but not DF508 CFTR inhibits Na^+ conductance when coexpressed in *Xenopus* oocytes. FEBS Lett 1996;381:47–52.
[13] Letz B, Korbmacher C. cAMP stimulates CFTR-like Cl^- channels and inhibits amiloride-sensitive Na^+ channels in mouse CCD cells. Am J Physiol 1997;272:C657–66.
[14] Jiang Q, Li J, Dubroff R, Ahn YJ, Foskett JK, Engelhardt J, et al. Epithelial sodium channels regulate cystic fibrosis transmembrane conductance regulator chloride channels in *Xenopus* oocytes. J Biol Chem 2000;275:13266–74.
[15] Konstas AA, Koch JP, Korbmacher C. cAMP-dependent activation of CFTR inhibits the epithelial sodium channel (ENaC) without affecting its surface expression. Pflügers Arch 2003;445(4):513–21.
[16] Nagel G, Barbry P, Chabot H, Brochiero E, Hartung K, Grygorczyk R. CFTR fails to inhibit the epithelial sodium channel ENaC expressed in *Xenopus laevis* oocytes. J Physiol 2005;564(Pt 3):671–82.
[17] Sheridan MB, Fong P, Groman JD, Conrad C, Flume P, Diaz R, et al. Mutations in the beta-subunit of the epithelial Na^+ channel in patients with a cystic fibrosis-like syndrome. Hum Mol Genet 2005;14(22):3493–8.
[18] Shimkets RA, Warnock DG, Bositis CM, Nelson-Williams C, Hansson JH, Schambelan M, et al. Liddle's syndrome: heritable human hypertension caused by mutations in the beta subunit of the epithelial sodium channel. Cell 1996;79(3):407–14.
[19] Bubien JK, Ismailow II, Berdiev BK, Cornwell T, Lifton RP, Fuller CM, et al. Liddle's disease: abnormal regulation of amiloride-sensitive Na^+ channels by b-subunit mutation. Am J Physiol 1996;270:C208–13.
[20] Chang SS, Grunder S, Hanukoglu A, Rosler A, Mathew PM, Hanukoglu I, et al. Mutations in subunits of the epithelial sodium channel cause salt wasting with hyperkalaemic acidosis, pseudohypoaldosteronism type 1. Nat Genet 1996;12(3):248–53.
[21] Hanukoglu A, Bistritzer T, Rakover Y, Mandelberg A. Pseudohypoaldosteronism with increased sweat and saliva electrolyte values and frequent lower respiratory tract infections mimicking cystic fibrosis. J Pediatr 1994;125(5 Pt 1):752–5.
[22] Marthinsen L, Kornfalt R, Aili M, Andersson D, Westgren U, Schaedel C. Recurrent Pseudomonas bronchopneumonia and other symptoms as in cystic fibrosis in a child with type I pseudohypoaldosteronism. Acta Paediatr 1998;87(4):472–4.
[23] Mall M, Grubb BR, Harkema JR, O'Neal WK, Boucher RC. Increased airway epithelial Na^+ absorption produces cystic fibrosis-like lung disease in mice. Nat Med 2004;10(5):487–93.
[24] Dagenais A, Gosselin D, Guilbault C, Radzioch D, Berthiaume Y. Modulation of epithelial sodium channel (ENaC) expression in mouse lung infected with *Pseudomonas aeruginosa*. Respir Res 2005;6(1):2.
[25] Blank U, Rückes C, Clauss W, Hofmann T, Lindemann H, Münker G, et al. Cystic fibrosis and non-cystic fibrosis human nasal epithelium show analogous Na^+ absorption and reversible block by phenamil. Pflügers Arch 1997;434:19–24.
[26] Rückes C, Blank U, Möller K, Rieboldt J, Lindemann H, Münker G, et al. Amiloride-sensitive Na^+ channels in human nasal epithelium are different from classical epithelial Na^+ channels. Biochem Biophys Res Commun 1997;237:488–91.
[27] Blank U, Clauss W, Weber W-M. Effects of benzamil in human cystic fibrosis airway epithelium. Cell Physiol Biochem 1995;5:385–90.
[28] Pfaffl MW. A new mathematical model for relative quantification in real-time RT-PCR. Nucleic Acids Res 2001;29(9):e45.

[29] Pfaffl MW, Horgan GW, Dempfle L. Relative expression software tool (REST) for group-wise comparison and statistical analysis of relative expression results in real-time PCR. Nucleic Acids Res 2002;30(9): e36.
[30] Hanwell D, Ishikawa T, Saleki R, Rotin D. Trafficking and cell surface stability of the epithelial Na^+ channel expressed in epithelial Madin–Darby canine kidney cells. J Biol Chem 2002;277(12): 9772–9.
[31] Bradford MM. A rapid and sensitive method for the quantitation of microgram quantities of protein utilizing the principle of protein-dye binding. Anal Biochem 1976;72:248–54.
[32] Abramoff MD, Magelhaes PJ, Ram SJ. Image processing with image. J Biophoton Int 2004;11(7):36–42.
[33] Walker NJ. Tech.Sight. A technique whose time has come. Science 2002;296(5567):557–9.
[34] Matsui H, Grubb BR, Tarran R, Randell SH, Gatzy JT, Davis CW, et al. Evidence for periciliary liquid layer depletion, not abnormal ion composition, in the pathogenesis of cystic fibrosis disease. Cell 1998;95:1005–15.
[35] Boucher RC. Evidence for airway surface dehydration as the initiating event in CF airway disease. J Intern Med 2007;261(1):5–16.
[36] Jayaraman S, Song Y, Vetrivel L, Shankar L, Verkman AS. Noninvasive in vivo fluorescence measurement of airway-surface liquid depth, salt concentration, and pH. J Clin Invest 2001;107:317–24.
[37] Kunzelmann K, Kathöfer S, Greger R. Na^+ and Cl-conductances in airway epithelial cells: increased Na^+ conductance in cystic fibrosis. Pflügers Arch-Eur J Physiol 1995;431:1–9.
[38] Hughey RP, Mueller GM, Bruns JB, Kinlough CL, Poland PA, Harkleroad KL, et al. Maturation of the epithelial Na^+ channel involves proteolytic processing of the alpha- and gamma-subunits. J Biol Chem 2003;278(39):37073–82.
[39] Hughey RP, Bruns JB, Kinlough CL, Harkleroad KL, Tong Q, Carattino MD, et al. Epithelial sodium channels are activated by furin-dependent proteolysis. J Biol Chem 2004;279(18):18111–4.
[40] Johnson MD, Bao HF, Helms MN, Chen XJ, Tigue Z, Jain L, et al. Functional ion channels in pulmonary alveolar type I cells support a role for type I cells in lung ion transport. Proc Natl Acad Sci U S A 2006;103(13):4964–9.
[41] Heijerman H. Infection and inflammation in cystic fibrosis: a short review. J Cyst Fibros 2005;4(Suppl 2):3–5.
[42] Myerburg MM, Butterworth MB, McKenna EE, Peters KW, Frizzell RA, Kleyman TR, et al. Airway surface liquid volume regulates ENaC by altering the serine protease-protease inhibitor balance: a mechanism for sodium hyperabsorption in cystic fibrosis. J Biol Chem 2006;281:27942–9.
[43] Terheggen-Lagro SW, Rijkers GT, van der Ent CK. The role of airway epithelium and blood neutrophils in the inflammatory response in cystic fibrosis. J Cyst Fibros 2005;4(Suppl 2):15–23.
[44] Kahl B, Herrmann M, Everding AS, Koch HG, Becker K, Harms E, et al. Persistent infection with small colony variant strains of *Staphylococcus aureus* in patients with cystic fibrosis. J Infect Dis 1998;177(4):1023–9.
[45] May A, Puoti A, Gaeggeler H-P, Horisberger J-D, Rossier BC. Early effect of aldosterone on the rate of synthesis of the epithelial sodium channel α subunit in A6 renal cells. J Am Soc Nephrol 1997;8: 1813–22.
[46] McNicholas CM, Canessa CM. Diversity of channels generated by different combinations of epithelial channel subunits. J Gen Physiol 1997;109:681–92.
[47] Farman N, Talbot CR, Boucher RC, Fay M, Canessa CM, Rossier BC, et al. Noncoordinated expression of α-, β-, and γ-subunit mRNAs of epithelial Na^+ channel along rat respiratory tract. Am J Physiol 1997;272:C131–41.
[48] Asher C, Wald H, Rossier BC, Garty H. Aldosterone-induced increase in the abundance of Na^+ channel subunits. Am J Physiol 1996;271: C605–11.
[49] Lingueglia E, Renard S, Waldmann R, Voilley N, Champigny G, Plass H, et al. Different homologous subunits of the amiloride-sensitive Na^+ channel are differently regulated by aldosterone. J Biol Chem 1994;269:13736–9.
[50] Ergonul Z, Frindt G, Palmer LG. Regulation of maturation and processing of ENaC subunits in the rat kidney. Am J Physiol Renal Physiol 2006;291(3):F683–93.
[51] Hofmann T, Stutts MJ, Ziersch A, Rückes C, Weber W-M, Knowles MR, et al. Effects of topically delivered benzamil and amiloride on nasal potential difference and sodium absorption in cystic fibrosis respiratory epithelium. Am J Respir Crit Care Med 1998;157:1844–9.
[52] Hirsh AJ, Sabater JR, Zamurs A, Smith RT, Paradiso AM, Hopkins S, et al. Evaluation of second generation amiloride analogs as therapy for cystic fibrosis lung disease. J Pharmacol Exp Ther 2004;311(3): 929–38.
[53] Arai K, Zachman K, Shibasaki T, Chrousos GP. Polymorphisms of amiloride-sensitive sodium channel subunits in five sporadic cases of pseudohypoaldosteronism: do they have pathologic potential? J Clin Endocrinol Metab 1999;84(7):2434–7.
[54] Saxena A, Hanukoglu I, Saxena D, Thompson RJ, Gardiner RM, Hanukoglu A. Novel mutations responsible for autosomal recessive multisystem pseudohypoaldosteronism and sequence variants in epithelial sodium channel alpha-, beta-, and gamma-subunit genes. J Clin Endocrinol Metab 2002;87(7):3344–50.
[55] Voilley N, Bassilana F, Mignon C, Merscher S, Mattei MG, Carle GF, et al. Cloning, chromosomal localization, and physical linkage of the beta and gamma subunits (SCNN1B and SCNN1G) of the human epithelial amiloride-sensitive sodium channel. Genomics 1995;28(3):560–5.
[56] McDonald FJ, Price MP, Snyder PM, Welsh MJ. Cloning and expression of the β- and γ-subunits of the human epithelial sodium channel. Am J Physiol 1995;268:C1157–63.